A Cramér-Rao Bound for Indoor Power Delay Profile Based Ranging ⋆

Fangqing Xiao, Dirk Slock

A Cramér–Rao Bound for Indoor Power Delay Profile Based Ranging*

Fangqing Xiao[1], Dirk Slock[1]

[1]Eurecom, Campus SophiaTech, 450 Route des Chappes, 06410 Biot, France

Abstract

Power Delay Profile (PDP) offers valuable insights into the propagation power fading of Line of Sight (LoS) and Non Line of Sight (NLoS) paths, making it a potential resource for ranging estimation. Despite its potential, the research on the lower bound of ranging error for PDP-based ranging is limited. This paper addresses this gap by introducing the Cramér–Rao bound (CRB) for Power Delay Profile (PDP) based ranging and Received Signal Strength Indicator (RSSI) based ranging, considering a specific indoor channel fading model. Through extensive simulations and analysis, we demonstrate the superiority of PDP-based ranging over RSSI-based ranging. Our findings contribute to a deeper understanding of the potential benefits of PDP-based ranging techniques.

Keywords

Cramér–Rao Bound, Power Delay Profile, Ranging Estimation, Received Signal Strength Indicator

1. Introduction

Ranging estimation plays a crucial role in localization for fifth-generation (5G) and beyond 5G (B5G) networks, finding applications in network planning, resource allocation, emergency services, and location-based services (LBS) [1]. While Received Signal Strength Indicator (RSSI) has been commonly used for ranging, the emergence of Wi-Fi and Orthogonal Frequency Division Multiplexing (OFDM) technology has led researchers to explore the potential of Power Delay Profile (PDP) for ranging estimation [2, 3, 4]. PDP provides more detailed information about the channel, including the fading amplitudes of Light-of-Sight (LoS) and Non-Light-of-Sight paths [5, 6].

While RSSI-based ranging offers an analytical approach for range estimation with minimal calibration parameters, it provides limited information compared to the comprehensive range details that can be extracted from the entire Channel Impulse Response (CIR). In order to enhance RSSI-based ranging, researchers such as K. Wu et al. [7] have harnessed Channel State Information (CSI) to develop a more precise propagation model. This approach has resulted in improved accuracy when compared to traditional RSSI-based methods. It's noteworthy that certain studies [8] have undertaken an analysis of the CRB for CSI-based localization. In their analysis, they preprocessed the CSI data to obtain the average intensity of CSI and delved into establishing a relationship between this average intensity and distance. It's worth mentioning

Proceedings of the Work-in-Progress Papers at the 13th International Conference on Indoor Positioning and Indoor Navigation (IPIN-WiP 2023), September 25 - 28, 2023, Nuremberg, Germany

fangqing.xiao@eurecom.fr (F. Xiao); dirk.slock@eurecom.fr (D. Slock)

that they solely focused on the first cluster but not other clusters, which typically contains propagation distance information. In contrast, our proposed approach diverges from theirs. We initiate range estimation by utilizing the Power Delay Profile (PDP) of identifiable multiple paths.

Our approach to PDP-based ranging involves utilizing the fading information of LoS and NLoS paths to estimate the LoS distance. The distance-dependent attenuation introduces an upper bound mask on the PDP, further influenced by random effects such as shadowing and reflection/diffraction. Therefore, building a statistical model that accounts for propagation distance and PDP is essential. Over the years, various models have been proposed for microwave signal propagation attenuation with respect to (w.r.t.) average power fading [9, 10, 11]. For instance, the Saleh-Valenzuela model [10] presents received signal rays arriving in clusters with independent uniform phases and independent Rayleigh amplitudes decaying exponentially with cluster and ray delays. Additionally, the relationship between average power attenuation and propagation distance has been studied in indoor and outdoor environments [12, 13, 14]. G. Steinböck et al. [13] proposed an indoor model incorporating a delay power spectrum with a primary component (early) following an inverse distance power law (d^{-n}) and a reverberant component (tail) decaying exponentially with distance for indoor environments. Based on these models, multi-path fading coefficients are expected to be correlated with propagation distances, with their magnitudes following a Rayleigh distribution whose variance depends on the LoS distance plus NLoS delay distance.

In this paper, we analyze the theoretical performance of the PDP-based ranging approach and the RSSI-based ranging approach using PDP with Saleh-Valenzuela model and the indoor model proposed by G. Steinböck et al, considering random shadowing, reflection/diffraction attenuation effects and the discrete nature of multipath. We derive the CRB for PDP-based range estimation via joint parameters estimation and marginalized range estimation for indoor environments. Furthermore, we present a novel CRB for range estimation based on RSSI by analyzing each path's fading under the selected propagation fading model rather than setting them as fixed numbers. Through simulation, we preliminarily verify that PDP-based ranging has better theoretical performance than RSSI-based ranging. This finding suggests that PDP-based ranging is worth exploring in different application scenarios.

This paper is organized as follows: In Section II, we introduce the OFDM model and the selected channel fading model. Sections III and IV delve into the joint parameters estimation CRB and the marginalized ranging estimation CRB for PDP-based ranging, respectively. In Section V, we derive the CRB of classical RSSI-based ranging. Section VI presents the simulation experiments and analysis of the results. Finally, in Section VII, we make a conclusion.

2. System Model

2.1. OFDM Model

The OFDM model we are considering assumes an OFDM symbol length of L, consisting of a Line-of-Sight (LoS) path and K Non-Line-of-Sight (NLoS) propagation paths. This model operates with a sampling period of T_s and an OFDM symbol period of T_0. One advantage the OFDM model is the elimination of need for precise knowledge of the pulse shape, as it makes

use of pilot subcarriers within the pulse shape's passband.

The received signal vector $\boldsymbol{y}$ in the OFDM system can be expressed as:

$$\boldsymbol{y} = \boldsymbol{X}\boldsymbol{T}\boldsymbol{a} + \boldsymbol{v} = \boldsymbol{H}\boldsymbol{a} + \boldsymbol{v}, \tag{1}$$

where the received signal vector $\boldsymbol{y} \in \mathcal{C}^{L\times 1}$ is defined as:

$$\boldsymbol{y} = \begin{bmatrix} y[s_1] \\ \vdots \\ y[s_L] \end{bmatrix}; \tag{2}$$

The matrix $\boldsymbol{X} \in \mathcal{C}^{L\times L}$ is filled with pilots and given by:

$$\boldsymbol{X} = \begin{bmatrix} X[s_1]e^{\frac{j2\pi s_1 T_0}{LT_s}} & \cdots & 0 \\ \vdots & \ddots & \vdots \\ 0 & \cdots & X[s_L]e^{\frac{j2\pi s_L T_0}{LT_s}} \end{bmatrix}; \tag{3}$$

The matrix $\boldsymbol{T} \in \mathcal{C}^{(L\times(K+1))}$ includes pulse shape filtered delayed path responses and is shown as:

$$\boldsymbol{T} = \begin{bmatrix} P[f_{s_1}]e^{\frac{-j2\pi s_1 \tau_0}{LT_s}} & \cdots & P[f_{s_1}]e^{\frac{-j2\pi s_1 \tau_K}{LT_s}} \\ \vdots & \ddots & \vdots \\ P[f_{s_L}]e^{\frac{-j2\pi s_L \tau_0}{LT_s}} & \cdots & P[f_{s_L}]e^{\frac{-j2\pi s_1 \tau_K}{LT_s}} \end{bmatrix}, \tag{4}$$

where τ and P represent the propagation delay and the pulse shape, respectively.

The vector $\boldsymbol{a} \in \mathcal{C}^{(K+1)\times 1}$ indicates the complex attenuation coefficient (amplitude $\boldsymbol{m} \in \mathcal{C}^{(K+1)}$ and phase $\boldsymbol{\phi} \in \mathcal{C}^{(K+1)}$) and is presented as:

$$\boldsymbol{a} = \begin{bmatrix} a_0 \\ \vdots \\ a_k \end{bmatrix} = \begin{bmatrix} m_0 e^{j\phi_0} \\ \vdots \\ m_k e^{j\phi_k} \end{bmatrix} = \mathcal{D}(\mathrm{e}^{j\boldsymbol{\phi}})\boldsymbol{m} = \mathcal{D}(\boldsymbol{m})\mathrm{e}^{j\boldsymbol{\phi}}, \tag{5}$$

where $\mathcal{D}(*)$ represents an operation that converts a vector to a diagonal matrix. The vector $\boldsymbol{v} \in \mathcal{C}^{L\times 1}$ is a complex Gaussian noise vector, and each element v_i follows a distribution $\mathcal{CN}(0, \sigma_v^2)$.

Firstly, we assume that each ϕ_i in $\boldsymbol{\phi}$ is an independent and identically distributed (i.i.d.) random variable drawn from a uniform distribution on the interval $[0, 2\pi)$.

Secondly, we consider the matrix $\boldsymbol{X}$ to be known and $\boldsymbol{T}$ to have been estimated prior to ranging estimation. Additionally, we presume that the estimation error of $\boldsymbol{T}$ is negligible, as this paper does not focus on examining its bias impact.

Furthermore, we assume that the multipath scenario includes distinguishable LoS path and NLoS paths. In this context, each delay τ_i between the i_{th} NLoS path and the LoS path is measurable with negligible error. This assumption is grounded in the understanding that the measurement of delays is considerably more accurate compared to the estimation of path complex amplitudes.

Additionally, we assume that the majority of the system's subcarriers are within the pulse shape's passband. In this region, the function $P(f)$ representing the pulse shape is approximately equal to 1. This assumption simplifies the model by considering that most subcarriers experience minimal distortion or attenuation within the passband.

2.2. Rayleigh Fading Amplitudes

According to the Saleh-Valenzuela model [5], by identifying the first ray of each cluster as the LoS path and the remaining rays as NLoS paths, the probability density function of the fading amplitude m_k for the k-th path can be described by a Rayleigh distribution:

$$f(m_k|\sigma_{d_k}^2) = \frac{2m_k}{\sigma_{d_k}^2} \mathrm{e}^{-\frac{m_k^2}{\sigma_{d_k}^2}}, \tag{6}$$

where $\sigma_{d_k}^2$ represents the average power gain of the k-th path. It is evident that $\sigma_{d_k}^2$ is associated with the propagation distance d_k of the k-th path.

2.3. LoS + Reverberating NLoS PDP Mode

According to the indoor model proposed by G. Steinböck et al. [6], the average power gain can be decomposed into the primary LoS component and the NLoS reverberating component. The gain of the LoS and NLoS paths at a distance d is given by:

$$G(d) = \begin{cases} G_0 \left(\frac{d_{\text{ref}}}{d}\right)^n; & \text{LoS}, \\ G_0 \left(\frac{d_{\text{ref}}}{d}\right)^n + G_{0,\text{rev}} T \mathrm{e}^{\frac{-d}{cT}}; & \text{NLoS}, \end{cases}, \tag{7}$$

where G_0 represents the gain at an arbitrary reference distance d_{ref}, $G_{0,\text{rev}}$ is the reference gain of the reverberant component, T is the reverberation time, c is the speed of light, and n is the environment path gain exponent.

For localization estimation, we assume that the values of G_0 and $G_{0,\text{rev}}$ at a reference distance of 1 meter and the value of T are known prior information. Therefore, for each path k with a distance d_k, the average expected gain $\sigma_{d_k}^2$ can be expressed as:

$$\sigma_{d_k}^2 = G(d_k) = \begin{cases} G_0 d_0^{-n}; & k = 0, \\ G_0 d_k^{-n} + G_1 \mathrm{e}^{\frac{-d_k}{cT}}; & k \neq 0, \end{cases} \tag{8}$$

where G_1 represents $G_{0,\text{rev}}T$. Furthermore, $\sigma_{d_k}^2$ in (6) is a specific expression of $G(d_k)$. Additionally, for each NLoS path distance d_k, it can be represented as:

$$d_k = d_0 + c\tau_k, \tag{9}$$

where τ_k is the delay time from the LoS path to the k-th NLoS path, and it is measurable with negligible error as previously hypothesized.

3. Joint Range Estimation CRB for PDP-Based Ranging

To model the LoS path distance d_0, we apply a Markov chain, disregarding any information about d_0 in $\boldsymbol{\phi}$ and $\boldsymbol{T}$. This means that we consider d_0 to be independent of the complex attenuation coefficients and the pulse shape filtered delayed path response.

By ignoring the information about d_0 in $\boldsymbol{\phi}$ and $\boldsymbol{T}$, we assume that the variations or dynamics of d_0 do not directly affect or depend on the complex attenuation coefficients or the pulse shape filtered delayed path response. Instead, the evolution of d_0 is modeled using a Markov chain, where the future values of d_0 only depend on its current state and not on its past states.

This simplification allows us to analyze the behavior of d_0 using the theory and techniques of Markov chains as

$$d_0 \rightarrow \boldsymbol{a} \rightarrow \boldsymbol{y}. \tag{10}$$

For the joint parameters estimation of $\boldsymbol{\theta} = [d_0, \boldsymbol{m}, \boldsymbol{\phi}]$, we can express the Fisher Information Matrix (FIM) as below:

$$\boldsymbol{FIM} = E_{\boldsymbol{y},\boldsymbol{m},\boldsymbol{\phi}}\left[-\frac{\partial^2 \log f(\boldsymbol{y},\boldsymbol{m},\boldsymbol{\phi}|d_0)}{\partial\boldsymbol{\theta}\partial\boldsymbol{\theta}^{\intercal}}\right] = E_{\boldsymbol{y},\boldsymbol{m},\boldsymbol{\phi}}\begin{bmatrix} J_{d_0 d_0} & J_{d_0 \boldsymbol{m}} & J_{d_0 \boldsymbol{\phi}} \\ J_{\boldsymbol{m} d_0} & J_{\boldsymbol{m}\boldsymbol{m}} & J_{\boldsymbol{m}\boldsymbol{\phi}} \\ J_{\boldsymbol{\phi} d_0} & J_{\boldsymbol{\phi}\boldsymbol{m}} & J_{\boldsymbol{\phi}\boldsymbol{\phi}} \end{bmatrix}, \tag{11}$$

where $\intercal$ is matrix transpose operator and the probability density function (pdf) $f(\boldsymbol{y}, \boldsymbol{m}, \boldsymbol{\phi}|d_0)$ can be expressed as follows:

$$f(\boldsymbol{y}, \boldsymbol{m}, \boldsymbol{\phi}|d_0) = f(\boldsymbol{y}|\boldsymbol{m}, \boldsymbol{\phi}) f(\boldsymbol{m}|d_0) f(\boldsymbol{\phi}). \tag{12}$$

Within the context of (12), it is possible to represent each pdf as follows:

$$f(\boldsymbol{y}|\boldsymbol{m}, \boldsymbol{\phi}) = \frac{1}{\pi^L \sigma_v^{2L}} \exp\left(-\frac{(\boldsymbol{y} - \boldsymbol{H}\mathcal{D}(\boldsymbol{m})\mathrm{e}^{j\boldsymbol{\phi}})^H (\boldsymbol{y} - \boldsymbol{H}\mathcal{D}(\boldsymbol{m})\mathrm{e}^{j\boldsymbol{\phi}})}{\sigma_v^2}\right), \tag{13}$$

$$f(\boldsymbol{m}|d_0) = \prod_{k=0}^{k=K} f(m_k|\sigma_{d_k}^2(d_0)) = \prod_{k=0}^{k=K} \frac{2m_k}{\sigma_{d_k}^2(d_0)} \mathrm{e}^{-\frac{m_k^2}{\sigma_{d_k}^2(d_0)}}, \tag{14}$$

$$f(\boldsymbol{\phi}) = \prod_{k=0}^{k=K} f(\phi_k) = \left(\frac{1}{2\pi}\right)^{K+1}. \tag{15}$$

where $()^H$ denotes the conjugate transpose. Upon logarithmically processing (12), we obtain:

$$\log f(\boldsymbol{y}, \boldsymbol{m}, \boldsymbol{\phi}|d_0) = \log f(\boldsymbol{y}|\boldsymbol{m}, \boldsymbol{\phi}) + \log f(\boldsymbol{m}|d_0) + \log f(\boldsymbol{\phi}). \tag{16}$$

Through the process of derivation, we can express each element inside (11) as follows:

$$J_{d_0 d_0} = -\frac{\partial^2 \log f(\boldsymbol{m}|d_0)}{\partial d_0^2}, \tag{17}$$

$$J_{d_0 \boldsymbol{m}} = J_{\boldsymbol{m} d_0}^{\intercal} = -\frac{\partial^2 \log f(\boldsymbol{m}|d_0)}{\partial d_0 \partial \boldsymbol{m}^{\intercal}}, \tag{18}$$

$$J_{d_0\boldsymbol{\phi}} = J_{\boldsymbol{\phi}d_0}^{\intercal} = -\frac{\partial^2 \log f(\boldsymbol{y}, \boldsymbol{m}, \boldsymbol{\phi}|d_0)}{\partial d_0 \partial \boldsymbol{\phi}^{\intercal}} = \mathbf{0}, \tag{19}$$

$$J_{\boldsymbol{m}\boldsymbol{m}} = -\frac{\partial^2 \log f(\boldsymbol{y}|\boldsymbol{m}, \boldsymbol{\phi})}{\partial \boldsymbol{m} \partial \boldsymbol{m}^{\intercal}} - \frac{\partial^2 \log f(\boldsymbol{m}|d_0)}{\partial \boldsymbol{m} \partial \boldsymbol{m}^{\intercal}}, \tag{20}$$

$$J_{\boldsymbol{\phi}\boldsymbol{\phi}} = -\frac{\partial^2 \log f(\boldsymbol{y}|\boldsymbol{m}, \boldsymbol{\phi})}{\partial \boldsymbol{\phi} \partial \boldsymbol{\phi}^{\intercal}} - \frac{\partial^2 \log f(\boldsymbol{\phi})}{\partial \boldsymbol{\phi} \partial \boldsymbol{\phi}^{\intercal}}, \tag{21}$$

$$J_{\boldsymbol{m}\boldsymbol{\phi}} = J_{\boldsymbol{\phi}\boldsymbol{m}}^{\intercal} = -\frac{\partial^2 \log f(\boldsymbol{y}|\boldsymbol{m}, \boldsymbol{\phi})}{\partial \boldsymbol{m} \partial \boldsymbol{\phi}^{\intercal}}. \tag{22}$$

Utilizing Equation (11), we can calculate the CRB of d_0 when performing joint parameters estimation:

$$CRB_{d_0} = \{E_{\boldsymbol{y},\boldsymbol{m},\boldsymbol{\phi}}[J_{d_0 d_0}] - E_{\boldsymbol{y},\boldsymbol{m},\boldsymbol{\phi}}[J_{d_0 \boldsymbol{m}}][E_{\boldsymbol{y},\boldsymbol{m},\boldsymbol{\phi}}[J_{\boldsymbol{m}\boldsymbol{m}}]]^{-1} E_{\boldsymbol{y},\boldsymbol{m},\boldsymbol{\phi}}[J_{\boldsymbol{m} d_0}]\}^{-1}. \tag{23}$$

The expectations w.r.t. $\boldsymbol{m}$, $\boldsymbol{\phi}$, and $\boldsymbol{y}$ inside (23) can be expressed as follows:

$$E_{\boldsymbol{y},\boldsymbol{m},\boldsymbol{\phi}} J_{\boldsymbol{m}\boldsymbol{m}} = \frac{2}{\sigma_v^2} diag(\boldsymbol{H}^H \boldsymbol{H} + \frac{1}{2}\boldsymbol{I}), \tag{24}$$

$$E_{\boldsymbol{y},\boldsymbol{m},\boldsymbol{\phi}} J_{d_0 d_0} = G_0\, n^2\, d_0^{-(n+2)} + \sum_{k=1}^{K} \left(\frac{n G_0 d_k^{-n-1} + \frac{G_1}{cT} \mathrm{e}^{\frac{-d_k}{cT}}}{G_0 d_k^{-n} + G_1 \mathrm{e}^{\frac{-d_k}{cT}}} \right)^2, \tag{25}$$

$$E_{\boldsymbol{y},\boldsymbol{m},\boldsymbol{\phi}} J_{d_0 \boldsymbol{m}} = E_{\boldsymbol{y},\boldsymbol{m},\boldsymbol{\phi}} J_{\boldsymbol{m} d_0}^{\intercal} = \left[n\pi d_0^{\frac{n-2}{2}} G_0^{-\frac{1}{2}}, \cdots, \frac{\sqrt{\pi} \left(\frac{G_0\, n}{d_k^{n+1}} + \frac{G_1\, \mathrm{e}^{-\frac{d_k}{T\, c}}}{T\, c} \right)}{\left(G_1\, \mathrm{e}^{-\frac{d_k}{T\, c}} + \frac{G_0}{d_k^n} \right)^{3/2}}, \cdots \right], \tag{26}$$

where $diag()$ is the operation of retaining the diagonal elements while setting all the non-diagonal elements to 0 of the matrix and $\boldsymbol{I}$ represents the identity matrix.

Having considered all the factors mentioned earlier, we can now proceed to calculate the joint estimation CRB for the estimation of d_0 w.r.t. PDP-based ranging:

$$\begin{aligned} CRB_{d_0} = \Bigg[& \sum_{k=1}^{K} \left(\frac{n G_0 d_k^{-n-1} + \frac{G_1}{cT} \mathrm{e}^{\frac{-d_k}{cT}}}{G_0 d_k^{-n} + G_1 \mathrm{e}^{\frac{-d_k}{cT}}} \right)^2 + G_0\, n^2\, d_0^{-(n+2)} - \frac{\sigma_v^2 \pi n^2 d_0^{(n-2)}}{2\, G_0} \left(\sum_{l=1}^{L} |h_{l0}|^2 + \frac{1}{2} \right)^{-1} \\ & - \frac{\sigma_v^2 \pi}{2} \sum_{k=1}^{K} \frac{\left(\frac{G_0\, n}{d_k^{n+1}} + \frac{G_1\, \mathrm{e}^{-\frac{d_k}{T\, c}}}{T\, c} \right)^2}{\left(G_1\, \mathrm{e}^{-\frac{d_k}{T\, c}} + \frac{G_0}{d_k^n} \right)^3} \left(\sum_{l=1}^{L} |h_{lk}|^2 + \frac{1}{2} \right)^{-1} \Bigg]^{-1}. \end{aligned} \tag{27}$$

4. Marginalized Range Estimation CRB for PDP-Based Ranging

According to (6), the NLoS path complex attenuation coefficients $\boldsymbol{a} \in \mathcal{C}^{(K+1)\times 1}$ that each element a_k is an i.i.d. complex zero-mean Gaussian random variable can be expressed as

follows:

$$\boldsymbol{a} \sim \mathcal{CN}(0, \boldsymbol{C_{aa}}), \quad \boldsymbol{C_{aa}} = \begin{bmatrix} \sigma_{d_0}^2 & \cdots & 0 \\ \vdots & \ddots & \vdots \\ 0 & \cdots & \sigma_{d_K}^2 \end{bmatrix}. \tag{28}$$

To estimate d_0 directly and solely based on $\boldsymbol{y} \in \mathcal{C}^{L\times 1}$, we can estabilish the pdf of $\boldsymbol{y}$ given $\boldsymbol{\sigma}^2(d_0) \in \mathcal{R}^{(K+1)\times 1}$ as follows:

$$f(\boldsymbol{y}|\boldsymbol{\sigma}^2(d_0)) = \pi^{-L}(\det(\boldsymbol{C_{yy}}))^{-1}\mathrm{e}^{-\boldsymbol{y}^H\boldsymbol{C_{yy}^{-1}}\boldsymbol{y}}, \tag{29}$$

where

$$\boldsymbol{C_{yy}} = \boldsymbol{H}\boldsymbol{C_{aa}}\boldsymbol{H}^H + \sigma_v^2\boldsymbol{I}, \quad \boldsymbol{\sigma}^2(d_0) = [\sigma_{d_0}^2 \ \cdots \ \sigma_{d_K}^2]^\intercal. \tag{30}$$

To compute the FIM from the pdf $f(\boldsymbol{y}|\boldsymbol{\sigma}^2(d_0))$, which is Gaussian with zero mean and covariance $\boldsymbol{C_{yy}}$, the FIM can be calculated as follows:

$$J_{d_0d_0} = (\frac{\partial\boldsymbol{\sigma}^2(d_0)}{\partial d_0})^\intercal \boldsymbol{J}_{\boldsymbol{\sigma}^2(d_0)\boldsymbol{\sigma}^2(d_0)}(\frac{\partial\boldsymbol{\sigma}^2(d_0)}{\partial d_0}). \tag{31}$$

For $\boldsymbol{J}_{\boldsymbol{\sigma}^2(d_0)\boldsymbol{\sigma}^2(d_0)}$, its element $\boldsymbol{J}_{\boldsymbol{\sigma}^2(d_0)\boldsymbol{\sigma}^2(d_0)_{i,k}}$ can be derived as:

$$J_{\boldsymbol{\sigma}^2(d_0)\boldsymbol{\sigma}^2(d_0)_{i,k}} = tr\left\{\boldsymbol{C_{yy}}\frac{\partial\boldsymbol{C_{yy}^{-1}}}{\partial\sigma_{di}^2}\boldsymbol{C_{yy}}\frac{\partial\boldsymbol{C_{yy}^{-1}}}{\partial\sigma_{dk}^2}\right\} = |\boldsymbol{e_i}^H\boldsymbol{H}^H\boldsymbol{C_{yy}^{-1}}\boldsymbol{H}\boldsymbol{e_k}|^2. \tag{32}$$

where $\boldsymbol{e}_i \in \mathcal{R}^{(K+1)\times 1}$ is a column vector with the i-th element being 1 and all other elements being 0. The trace operation, denoted by $tr(\cdot)$, computes the sum of the diagonal elements of a matrix. With these definitions, we can compute the FIM as follows:

$$\boldsymbol{J}_{\boldsymbol{\sigma}^2(d_0)\boldsymbol{\sigma}^2(d_0)} = (\boldsymbol{H}^H\boldsymbol{C_{yy}^{-1}}\boldsymbol{H}) \odot (\boldsymbol{H}^H\boldsymbol{C_{yy}^{-1}}\boldsymbol{H})^*, \tag{33}$$

where $\odot$ represents the Hadamard product (element-wise multiplication) and * denotes the conjugate operation. And

$$\frac{\partial\boldsymbol{\sigma}^2(d_0)}{\partial d_0} = \left[\frac{\partial\sigma_{d_0}^2}{\partial d_0} \ \cdots \ \frac{\partial\sigma_{d_K}^2}{\partial d_0}\right]^\intercal, \tag{34}$$

where k_{th} element can be presented as:

$$\frac{\partial\sigma_{dk}^2}{\partial d_0} = \begin{cases} -nG_0d_0^{-n-1}, & k = 0, \\ -nG_0d_k^{-n-1} - \frac{G_1}{cT}\mathrm{e}^{\frac{-d_k}{cT}}, & k \neq 0. \end{cases} \tag{35}$$

In conclusion, with (27) (28) and (29), the marginalized CRB of d_0 w.r.t. PDP-based ranging can be calculated as follows:

$$CRB_{d_0} = \left[(\frac{\partial\boldsymbol{\sigma}^2(d_0)}{\partial d_0})^\intercal \boldsymbol{J}_{\boldsymbol{\sigma}^2(d_0)\boldsymbol{\sigma}^2(d_0)}(\frac{\partial\boldsymbol{\sigma}^2(d_0)}{\partial d_0})\right]^{-1}. \tag{36}$$

5. CRB FOR Classical RSSI-Based Ranging

In the case where all data subcarriers can be used and considering the channel model, the RSSI can be measured from the squared Euclidean norm of the magnitude vector $\boldsymbol{y}$. Taking into account the law of large numbers, we can express $\|\boldsymbol{y}\|^2$ as:

$$\|\boldsymbol{y}\|^2 = E_v\|\boldsymbol{y}\|^2, \tag{37}$$

which represents the sum of squared magnitudes of the individual subcarriers.

Utilizing the squared Euclidean norm, the RSSI measurement provides an aggregate measure of the received signal strength across all the subcarriers, enabling an overall assessment of the signal power.

Since we assume that most of the subcarriers used for transmission are within the passband of the pulse slope where $P(f) \approx 1$, $E_v\|\boldsymbol{y}\|^2$ can be derived to:

$$E_V\|\boldsymbol{y}\|^2 = \alpha\|\boldsymbol{a}\|^2 + \beta = (\textstyle\sum_{i=1}^{L} X_i^2)\|\boldsymbol{a}\|^2 + L\sigma_v^2, \tag{38}$$

where

$$\|\boldsymbol{a}\|^2 = \textstyle\sum_{k=0}^{K} |a_k|^2 = \sum_{k=0}^{K}(a_k^{re2} + a_k^{im2}). \tag{39}$$

Using pilots to estimate the channel and perform interference cancellation, the complex attenuation coefficient $a_k = a_k^{re} + ja_k^{im}$ can be decomposed into its real part a_k^{re} and imaginary part a_k^{im}, both of which are Gaussian random variables. Specifically, we have $a_k^{re} \sim \mathcal{N}(0, \frac{\sigma_k^2}{2})$ and $a_k^{im} \sim \mathcal{N}(0, \frac{\sigma_k^2}{2})$.

For the LoS path ($k = 0$) and NLoS paths ($k \neq 0$), the variances σ_k^2 of the complex attenuation coefficients can be given as follows:

- For the LoS path ($k = 0$):
$$\sigma_0^2 = G_0 d_0^{-n}; \tag{40}$$
- For the NLoS paths ($k \neq 0$):
$$\sigma_k^2 = G_0 d_k^{-n} + G_1 \mathrm{e}^{\frac{-d_k}{cT}}, \tag{41}$$

where G_0 is the gain at an arbitrary reference distance d_{ref}, G_1 is the reference gain of the reverberant component, n is the environment path gain exponent, c is the speed of light, and T is the reverberation time. The variables d_0 and d_k represent the distances of the LoS path and NLoS paths, respectively.

Therefore, the real part a_k^{re} and imaginary part a_k^{im} of a_k are Gaussian random variables with variances $\frac{\sigma_k^2}{2}$, where σ_k^2 is given by the expressions mentioned above. If we assume that the real part a_k^{re} and imaginary part a_k^{im} of a_k have the same variance σ_0^2 for all k, then the magnitude squared $\|\boldsymbol{a}\|^2$ follows a Chi-squared distribution with $2(K+1)$ degrees of freedom. The probability density function (PDF) of the random variable $z = |\boldsymbol{a}|^2$ given σ_0 can be expressed as:

$$f_{(2K+2)}(z|\sigma_0^2) = \frac{z^K e^{-\frac{z}{\sigma_0^2}}}{\sigma_0^{2(K+1)}\Gamma(K+1)}, \tag{42}$$

Parameter	Value
SNR	range from 10 dB to 60 dB, default 20 dB.
L	30
n	ranging from 2.0 to 2.5, default 2.0.
K	random between 10 and 15.
d_0 (m)	20
distance of NLOS path (m)	random between $1.1d_0$ to $2.0d_0$.
G_0	1
G_1	1
T (ns)	20

Table 1: Parameters setting

where $\Gamma()$ is Gamma function and d_{ref} is chosen as 1 meter. Replacing σ_0^2 by a function of d_0, we can rewrite the pdf of the random variable $z = \|\boldsymbol{a}\|^2$ as:

$$f_{(2K+2)}(z|d_0) = \frac{z^K e^{-\frac{z}{G_0(\frac{1}{d_0})^n}}}{\left((G_0(\frac{1}{d_0})^n\right)^{(K+1)} \Gamma(K+1)}. \tag{43}$$

Additionally, it is easily to get:

$$E_Z(z) = \sigma_0^2(K+1). \tag{44}$$

Then we can calculate CRB of estimating d_0 from $\|\boldsymbol{a}\|^2$ w.r.t. classical RSSI-based ranging as

$$CRB_{d_0} = \frac{d_0^2}{n^2(K+1)}. \tag{45}$$

6. Simulation Results

In this section, we utilize MATLAB to compute the CRB for PDP-based ranging using joint parameter estimation and marginalized range estimation, as well as classical RSSI-based ranging. Our simulations incorporate the indoor radio propagation model introduced in Section II, which accounts for reverberating effects and path decay. The key parameters employed in the simulations are outlined in Table 1.

To investigate the factors influencing localization error, we focus on two primary factors: the Signal-to-Noise Ratio (SNR) of the channel and the path gain exponent. For each factor, we keep all other parameters at their default values and conduct the simulation to observe the behavior of the CRB.

The obtained performance results are presented in two figures. Figure 1 illustrates the behavior of the square root of the CRB for PDP-based ranging as the SNR increases from 10 dB to 60 dB. As expected, the root of the CRB decreases with higher SNR, indicating improved ranging accuracy due to the higher quality of the received signal. Notably, the performance of PDP-based ranging surpasses that of RSSI-based ranging. Moreover, marginalized range estimation demonstrates superior performance compared to joint estimation.

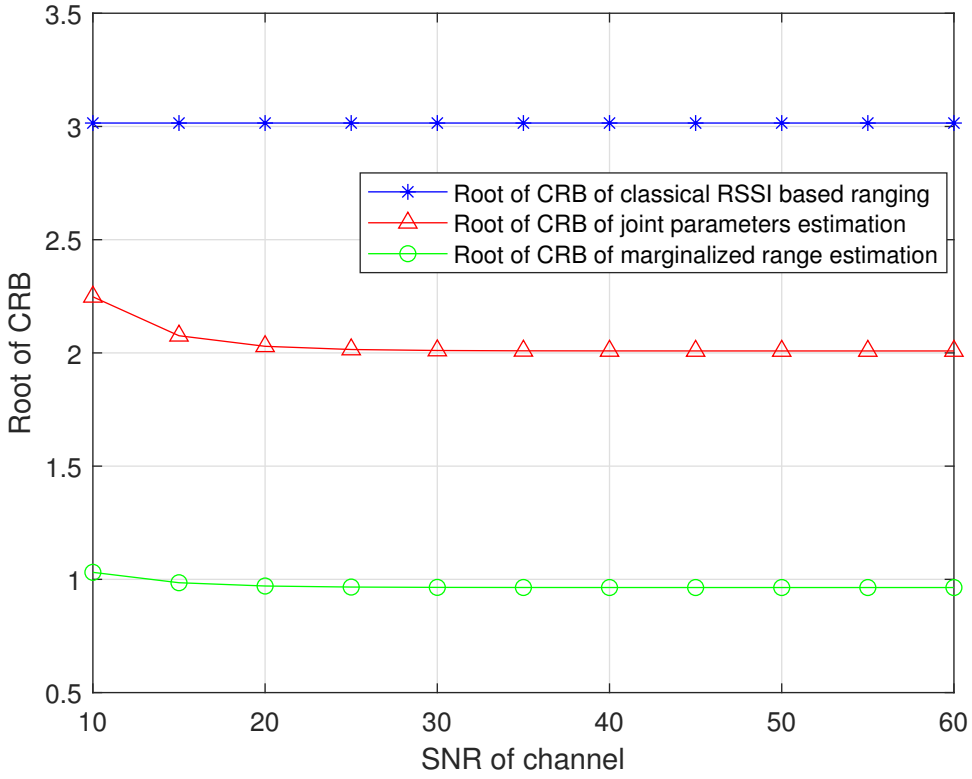

Figure 1: Comparision under different SNR.

Figure 2 compares the CRBs of PDP-based ranging and RSSI-based ranging for various path gain exponents. As the path gain exponent increases, indicating more complex propagation environments, all CRBs decrease. However, PDP-based ranging exhibits better theoretical performance than RSSI-based ranging across all path gain exponents. This suggests that PDP-based ranging can deliver favorable performance even in complex environments, making it a promising technique for localization applications. Furthermore, marginalized range estimation outperforms joint estimation in terms of localization accuracy.

These findings highlight the advantages of PDP-based ranging and marginalized range estimation, supporting their potential for accurate localization in diverse scenarios.

7. Concluding Remarks

In summary, this paper presents a comprehensive analysis of the Cramer-Rao Bound (CRB) for PDP-based positioning using both joint estimation and marginalized range estimation, as well as RSSI-based localization. The derived CRB takes into account the distance-dependent path decay of both Line-of-Sight (LoS) and Non-Line-of-Sight (NLoS) paths. The study investigates the impact of various factors on the CRB, including the Signal-to-Noise Ratio (SNR) of the

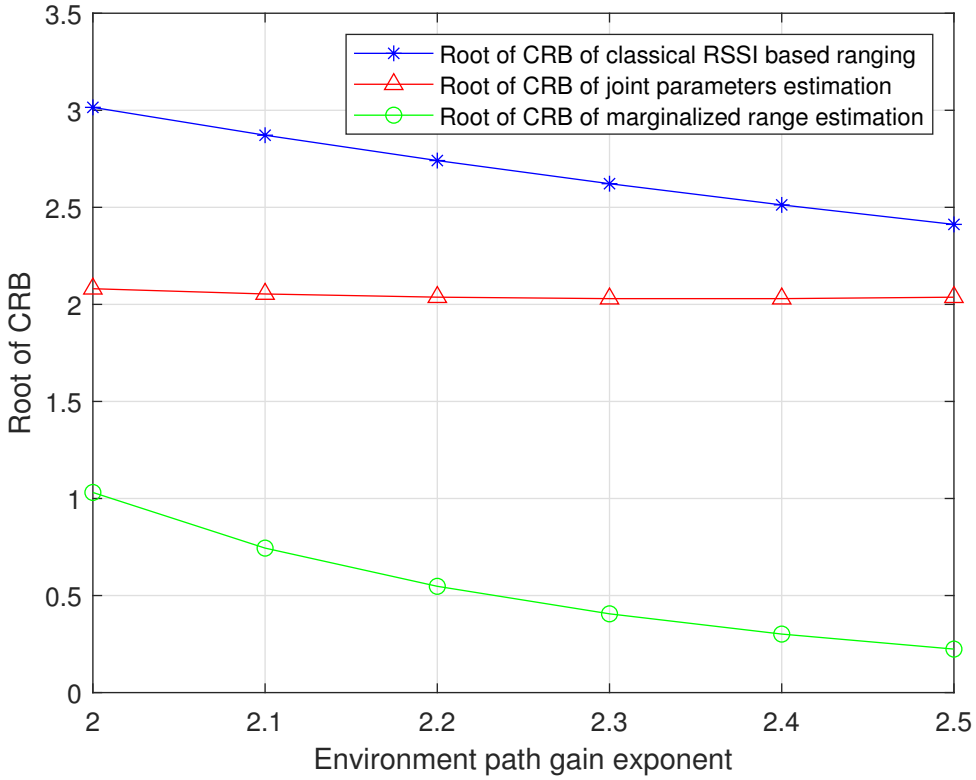

Figure 2: Comparision under different path gain exponent.

channel and the path gain exponent in different environments. The simulation results highlight the superiority of PDP-based localization over RSSI-based localization, with PDP-based ranging achieving better performance across different environments. Furthermore, the marginalized range estimation approach demonstrates improved accuracy compared to joint estimation. These findings contribute to the understanding of PDP-based localization and provide insights into its potential for accurate positioning in real-world scenarios.

Acknowledgements This research is partially supported by the French-Germany project 5G-OPERA.

References

[1] F. Mogyorósi, P. Revisnyei, A. Pašić, Z. Papp, I. Törös, P. Varga, A. Pašić, Positioning in 5g and 6g networks—a survey, Sensors 22 (2022).

[2] V. B. Vales, T. Dominguez-Bolano, C. J. Escudero, J. A. Garcia-Naya, Using the power delay profile to accelerate the training of neural network-based classifiers for the identification of los and nlos uwb propagation conditions, IEEE Access 8 (2020) 220205–220214.

[3] G. Ding, P. Chen, J. Tian, Q. Zhao, Power delay profile based indoor fingerprinting localization system, in: Proc. IEEE ICACT, 2016, pp. 324–329.
[4] T. Öktem, D. Slock, Power delay doppler profile fingerprinting for mobile localization in nlos, in: Proc. IEEE PIMRC, 2010, pp. 876–881.
[5] T. Cui, C. Tellambura, Power delay profile and noise variance estimation for ofdm, IEEE Commun. Lett. 10 (2006) 25–27.
[6] Y. Ai, M. Cheffena, Q. Li, Power delay profile analysis and modeling of industrial indoor channels, in: Proc. IEEE EUCAP, 2015, pp. 1–5.
[7] K. Wu, J. Xiao, Y. Yi, D. Chen, X. Luo, L. M. Ni, Csi-based indoor localization, IEEE Trans. Parallel Distrib. Syst. 24 (2012) 1300–1309.
[8] L. Gui, M. Yang, H. Yu, J. Li, F. Shu, F. Xiao, A cramer–rao lower bound of csi-based indoor localization, IEEE Trans. Veh. Technol. 67 (2017) 2814–2818.
[9] G. L. Turin, F. D. Clapp, T. L. Johnston, S. B. Fine, D. Lavry, A statistical model of urban multipath propagation, IEEE Trans. Veh. Technol. 21 (1972) 1–9.
[10] A. A. Saleh, R. Valenzuela, A statistical model for indoor multipath propagation, IEEE J. Sel. Areas Commun. 5 (1987) 128–137.
[11] S. Sun, T. A. Thomas, T. S. Rappaport, H. Nguyen, I. Z. Kovacs, I. Rodriguez, Path loss, shadow fading, and line-of-sight probability models for 5g urban macro-cellular scenarios, in: Proc. IEEE Globecom Workshops, 2015, pp. 1–7.
[12] J. Ko, Y.-J. Cho, S. Hur, T. Kim, J. Park, A. F. Molisch, K. Haneda, M. Peter, D.-J. Park, D.-H. Cho, Millimeter-wave channel measurements and analysis for statistical spatial channel model in in-building and urban environments at 28 ghz, IEEE Trans. Wirel. Commun. 16 (2017) 5853–5868.
[13] G. Steinböck, T. Pedersen, B. H. Fleury, W. Wang, R. Raulefs, Distance dependent model for the delay power spectrum of in-room radio channels, IEEE Trans. Antennas Propag. 61 (2013) 4327–4340.
[14] B. E. Bilgin, V. C. Gungor, Performance comparison of ieee 802.11 p and ieee 802.11 b for vehicle-to-vehicle communications in highway, rural, and urban areas, Int. J. Veh. Technol. 2013 (2013) 1–10.